IL NUOVO CIMENTO Vol. 36 C, N. 4 Luglio-Agosto 2013
DOI 10.1393/ncc/i2013-11540-4

Communications: SIF Congress 2012

The CHArged ANTI Counter for the NA62 experiment at CERN SPS

D. Di Filippo
Università di Napoli "Federico II" and INFN, Sezione di Napoli - Napoli, Italy

ricevuto il 31 Dicembre 2012

Summary. — The NA62 experiment at CERN is intended to measure, with 10% relative error, the Branching Ratio of the K decay $K^+ \to \pi^+\nu\bar{\nu}$ which is expected to occur only in about 8 out 10^{11} kaon decays. The measurement strategy is to detect the decaying kaon and its product π^+ and to reject all the background channels, which are up to ten orders of magnitude more abundant than the signal, using both kinematical constraints and particle identification systems as veto. The exceptionally low signal yield makes it necessary to prevent also background which is not due to kaon decays, but is rather connected to the interaction of the intense hadron beam with the residual material enconuntered along the decay volume including the beam spectrometer itself: in order to reduce to an acceptable level this last background we designed the Charged Anti Counter (CHANTI). CHANTI is designed to be a compact, efficient and fast response detector to be operated in vacuum and is made up assembling FNAL-NICADD scintillator bars and fast wavelength shifter fibers. It is read out via silicon photomultipliers coupled to fast electronics. It is composed by 6 stations with x-y views and tracking capability. We already constructed and characterized the bars for two stations and we fully assembled the first station. We also developed, in the NA62 framework (based on the GEANT4 package), a Monte Carlo simulation of the CHANTI and we got an estimation of its efficiency.

PACS 13.20.Eb – Decays of K mesons.
PACS 12.15.Hh – Determination of Cabibbo-Kobayashi & Maskawa (CKM) matrix elements.
PACS 12.60.-i – Models beyond the standard model.

1. – The NA62 experiment

The purpose of NA62 experiment is to measure the Branching Ratio (BR) of the K decay $K^+ \to \pi^+\nu\bar{\nu}$. The Standard Model prediction of this BR is very accurate (BR $= (8.5 \pm 0.7) \times 10^{-11}$, [1]) and it is very interesting to be measured because this process is quite sensitive to the flavour structure of possible new physics beyond the Standard Model [2, 3]. The current measurement of this BR is $1.73^{+1.15}_{-1.05} \times 10^{-10}$, performed by E787/E949 collaboration at Brookhaven National Laboratory [4].

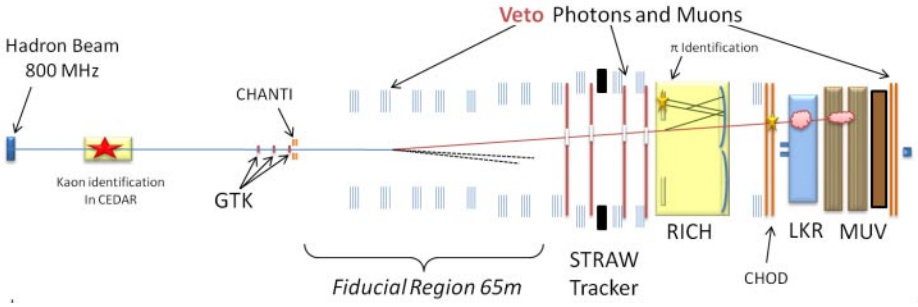

Fig. 1. – NA62 detector layout.

NA62 aims to collect $\sim$ 100 events in 2 year and to get a 10% background/signal ratio [5, 6]. The strategy is to generate an high-intensity K beam, to detect both the decaying kaon and the final π^+ coming from a big fiducial volume ($\approx$ 65 m), and to exclude all the other channels. In fig. 1 there is a scheme of the apparatus.

The K beam arises from a 400 GeV proton beam hitting on a berillium target (CERN T10 line). Then the beam optics selects particles with an average momentum of 75 GeV/c producing a 750 MHz unseparated positive hadron beam with a 6% kaon component. This system will be able to produce $\approx 4.8 \times 10^{12}$ K decays per year starting at the end of year 2014.

K is identified by a differential Cherenkov detector (CEDAR) while the final π^+ is identified in a Ring Imaging Cherenkov (RICH) and its momentum is measured in a Straw Chamber Spectrometer (STRAW). To exclude the other decays, there are an electromagnetic calorimeter (LKr) and several veto counters: large angle photon vetoes (LAV), low angles vetoes (IRC and SAC), muon veto detectors (MUV1-2-3).

In order to apply kinematical rejection [6] we need to measure the K momentum, to this aim we use a silicon-tracker–based spectrometer (the so-called GigaTracKer - GTK) to precisely measure the beam momentum and timing. However, the interaction of the beam with the GTK is itself a possible source of background. In particular, inelastic scattering events can mimic the signal if a produced pion falls into the RICH acceptance, if it is badly reconstructed inside the fiducial volume, and if no other tracks are detected.

The charged anti counter (CHANTI) is a detector placed in vacuum just after the GTK (27 mm) to help the rejection of this background, by covering hermetically the region between 49 mrad and 1.2 rad wrt the third and last GTK station. This detector is being designed, constructed and tested in Naples.

2. – CHANTI design

The CHANTI has to fulfill the following requirements:

- high efficiency for charged particles,
- maximum sustainable rate of the order of some kHz/cm^2,
- time resolution at nanosecond level to have a fake veto rate not exceeding 1–2% of the signal,
- radiation hardness up to some Gy/year,
- low outgassing rate and low power consumption to operate in vacuum.

A minor issue is the capability to perform some particle tracking in order to validate our inelastic event simulation and to study the beam halo. This will also improve the time resolution allowing to correct the raw times for xy position time offsets.

To meet these requirements we chose for the CHANTI plastic scintillators bars with a TiO_2 coating and a polystyrene core doped with fluorescent compound (blue emitting, 1% PPO and 0.03% POPOP). Their main characteristics are: good light yield (100% of Kuraray SCSN-81), radiation hardness (5% light yield loss for 1Mrad irradiation), fast response (1–2 ns). They are produced at FNAL-NICADD [7] and used, for example, by the MINERVA [8] and D0 [9] collaborations.

The bars have a cross-section of an isosceles-rectangle triangle shape with the hypotenuse of 33 mm. Each bar has a 1.7 mm diameter hole running along the bar to hold an optical fiber. We chose a fast wavelength shifting fiber (2.7 ns of remitting mean time, Saint-Gobain BCF-92 [10]). We read the fiber from one side while the other side is mirrored, using the same technique (Al sputtering in vacuum) developed for the ALICE calorimeter [11]. To collect the light and amplify the signal we chose Hamamatsu $1.3 \times 1.3\,\mathrm{mm}^2$ silicon photomultipliers (SiPM). The use of this kind of device is becoming a widespread solution in particle detectors where a high number of channels or high level of integration is needed [12-14]. They are intrinsically radiation hard device for MIPs and gammas, however there is a known issue with their behavior after intense neutron flux irradiation [15]. We checked trough simulation that it will not be a major issue in our environment [16].

The CHANTI is made of 6 stations of $30 \times 30\,\mathrm{cm}^2$, with x-y views and a $95 \times 65\,\mathrm{mm}^2$ hole in the center to leave room for the beam. Each view is made of two planes with bars arranged as in fig. 3, so a track passes trought 2 bars per view. It allows us to use the center of charge method and to improve spatial resolution and tracking performance.

We carefully chose the distance between each station and the GTK, so the CHANTI will be able to cover all the angles from 1.2 rad to 49 mrad. The angles from 49 mrad onward are covered by other detectors of the NA62 layout (*e.g.*, LAV, LKr etc.).

For the powering and reading of the SiPM, we developed in collaboration with Laboratori Nazionali di Frascati an all-in-one solution. Each board is a standard VME 9U with CAN interface and it can control up to 32 SiPM:

- it independently power up every SiPM by setting voltage bias with 10 mV precision;
- it can read absorbed current with few nA precision,
- it has a very good temperature stability (25 ppm/K),
- it has a fast signal amplification ($\times 25$),
- it can read temperature through pt100 probes.

The analog signal generated by this board will be processed by a Time Over Threshold board already designed for the LAV detector of NA62 [5]. For the digitization we will use the standard NA62 data acquisition chain: a fast TDC (100 ps resolution) and a dedicated board powered by 5 Altera FPGA that fetch the data and send it to the farm pc through fast ethernet [17].

3. – CHANTI construction

The construction phase starts by cutting the scintillator bars at 3 different lengths: 30 cm ("Long" bars), 11.75 cm ("Medium" bars) and 10.25 cm ("Short" bars). One side

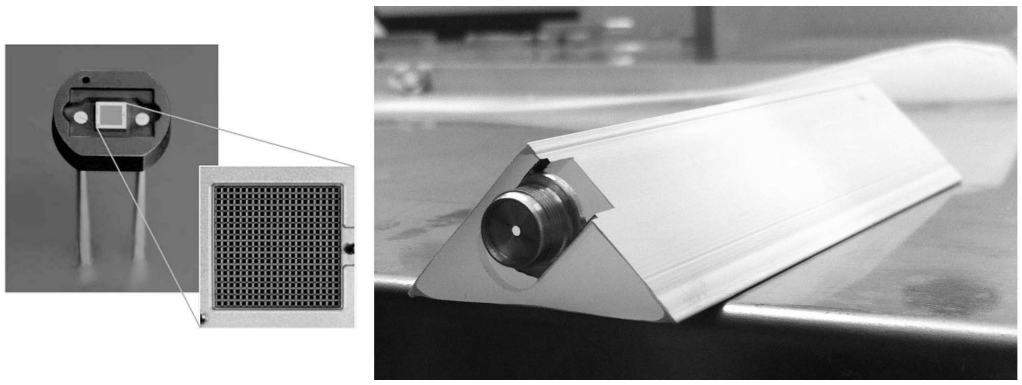

Fig. 2. – Left: Hamamatsu SiPM. Right: a fully assembled bar.

of each bar was machined to create the seat of the connector coupling the fiber to the SiPM (fig. 2).

Fibers are mirrored at one side (opposite to SiPM), cut at the right length and glued to the connectors. Then, each fiber is inserted in the hole of the scintillator bar, kept vertical by a dedicated support. The free space between the fiber and the scintillator is filled by an optical glue (GE Silicones - Silicone Elastomer), injected slowly from the bottom to prevent air mixing. The glue was previously placed in a vacuum pump to extract the air in it that otherwise could create bubbles during the fixing.

A structural glue (Epoxy 3MDP490) is used to fix the connector to the scintillator. The final aspect of the bar is shown in fig. 2.

When all the bars are ready, we perform a quality check (see sect. **5**) and a characterization of each of them. We also characterize every SiPM (see sect. **4**).

After the tests, we used an alignment jig and the structural glue to assemble the station; the result is shown in fig. 3. At the end the station is housed in an aluminum frame and the SiPM are placed in their connectors. Since the SiPMs could be damaged by relatively small force applied to their pins we designed a cabling solution based on a custom connector, a frame support and nylon bands. The first station, fully assembled,

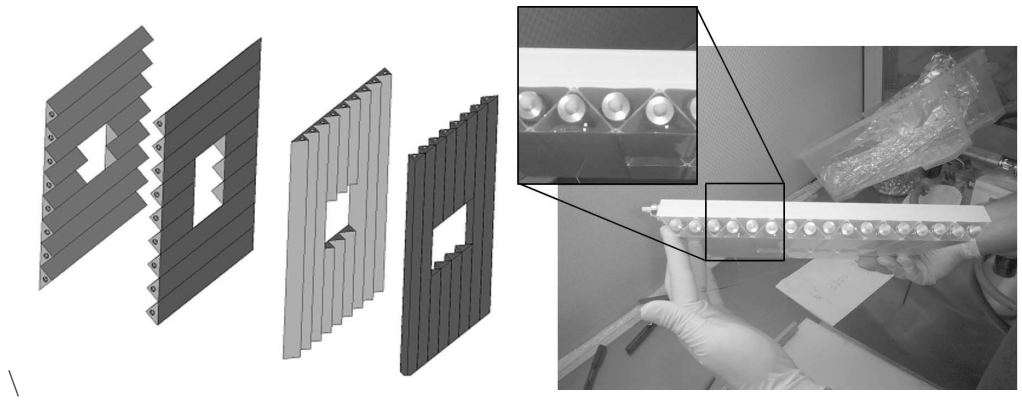

\

Fig. 3. – Left: CHANTI station layout. Right: station prototype just assembled.

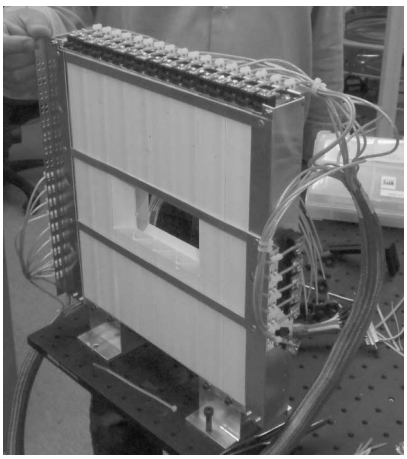

Fig. 4. – First station with mechanical frame and full cabling.

is shown in fig. 4. Thanks to the adoption of appropriate design features and material choices, the overall outgassing of one station has been kept very low: it has been measured to be less than $3 \cdot 10^{-5}$ mbar l/s. All the construction procedure takes about 20 days per station.

4. – SiPM characterization

The SiPM gain (and so the output signal height) depends linearly on $V - V_{bd}$, where V is the voltage applied to the SiPM (70V is a typical value) and V_{bd} is the breakdown voltage. So we need to know and monitor V_{bd} which is a function of temperature (69.5 V is a typical value at 20 °C). We can do this using the Voltage-Current response of the SiPM. Near the breakdown region, this curve is approximated by $I = \alpha(V - V_{bd})^2$ where I is the absorbed current. So we can measure V_{bd} by a fit to the $V - I$ curve. We designed an automatic system to test 32 SiPM at the same time; it uses a power supply with a nano-amperometer and an analog multiplexer, both controlled by a computer and LabView software. We performed the test in thermal chamber at 3 different temperatures: 20, 25 and 15 °C while the Hamamatsu specifies the SiPM properties only at 25 °C. The result for the first 36 SiPM used in the NA62 technical run in November 2012 are shown in fig. 5. In the final NA62 setup we will be able to routinely check $V - I$ curves online through the control electronics.

5. – Bars characterization

Once bars are glued inside the station they cannot be substituted if faulty. In order to get the required level of efficiency we have to check the response of each individual bar before assembling the detector. We did thus checks using cosmic rays. As the low rate of events did not allow for a study of the response of the bars as a function of the longitudinal coordinate, we performed two kind of tests.

In the first kind of test, the signal, read by a simple circuit, was sent to a large bandwidth, $\approx 11\times$, amplifier and the whole waveform was acquired using a fast digital oscilloscope connected to a pc. The test was performed in auto-trigger mode: we acquired

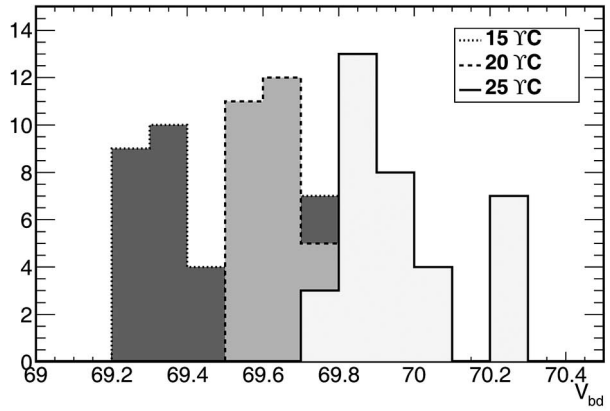

Fig. 5. – Breakdown voltage of the SiPM of the first station measured at 3 temperatures.

each event with a signal higher than 50 mV. This threshold was chosen in order to have an acquisition rate dominated by cosmic ray signals, in fact, with this threshold, the contribution from electronic noise and SiPM thermal noise is negligible (at level of %). The bars and electronics were put in a thermal chamber that allowed us to perform the test at a constant and fixed temperature of 25 °C. With this test we studied the global response of the bar. Smaller (larger) signals were mostly due to cosmic muons crossing the bar perpendicularly (non-perpendicularly) to its axis. As a variable to be used for the quality check we computed the ratio R of the number of signals exceeding 150 mV over the total.

In the second kind of test, the apparatus was the same but we had also two small scintillators and phototubes above the bars which form a telescope, in order to select almost straight cosmic rays passing next to the edge of the bar opposite to the SiPM. We acquired the signal only when there was a coincidence between the signals of the two phototubes. In this way we can have an idea of the response of the bar to a roughly vertical MIP muon, in the worst case scenario wrt to the fiber attenuation. For this kind of test we expressed the result as the mean number of generated photoelectrons N_{pe} which was obtained comparing the signal to the single photoelectron signal, that was previously determined for each SiPM in a dedicated run without bars measuring the dark noise.

We plotted R *vs.* N_{pe} for the first 96 bars in fig. 6. In this figure the two triangles refer to two "Reference" bars intentionally produced following a "Wrong" procedure: one without the optical glue and the other with a bad glue process (we let the glue to flow out during the fixing obtaining a non-uniform gluing). The ellipses shown in fig. 6 correspond to the 1σ, 2σ and 3σ contours obtained after a rotation to find out the two uncorrelated variables. We decided to reject all the bars underperforming out of 2σ contour.

In fig. 7 it is shown the time resolution obtained in an external triggering test with a long bar. In order to reach this resolution (≈ 0.9 ns), we need to apply time-slewing correction to the signal. This correction is based on a functional dependence of the time over threshold versus the delay between the signals of the bars and the triggers. We extracted this dependence by means of a fit performed over a sample data acquired during the tests.

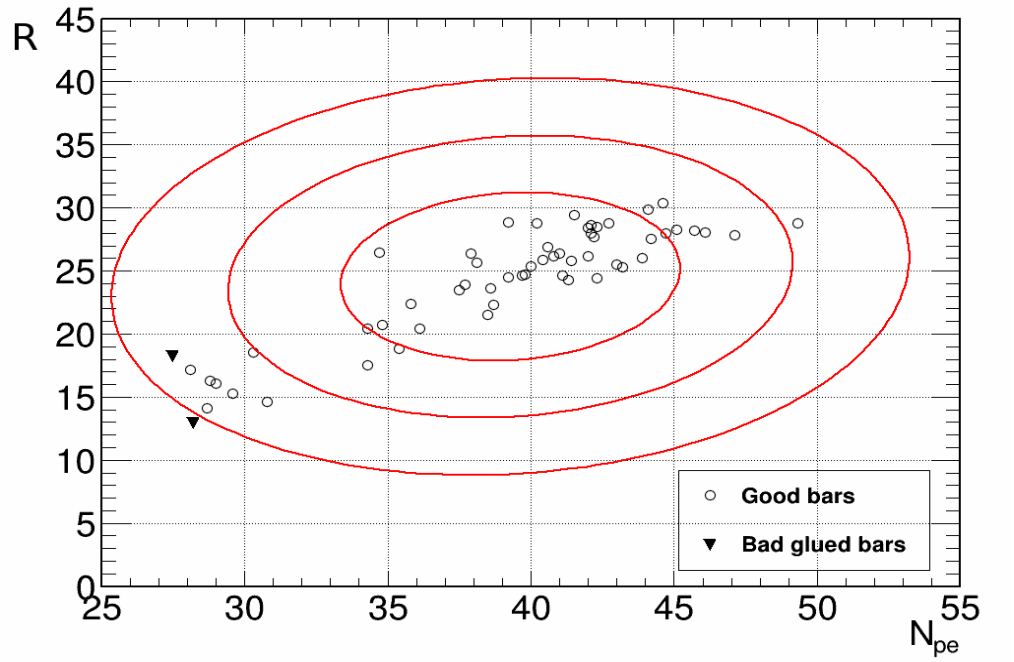

Fig. 6. – Autotrigger R *versus* external-trigger N_{pe} for the first 96 bars. The ellipses represent the 1σ, 2σ and 3σ bound. The triangles are the bad glued bars.

A perpendicular muon track always crosses two neighboring opposed bars. We report in fig. 7 the sum (over all the channels) of the collected charge in terms of number of photoelectron. This was obtained by a 5 bar prototype using an external cosmic ray trigger and by reading two opposite bars by a prototype electronics and a digital oscilloscope.

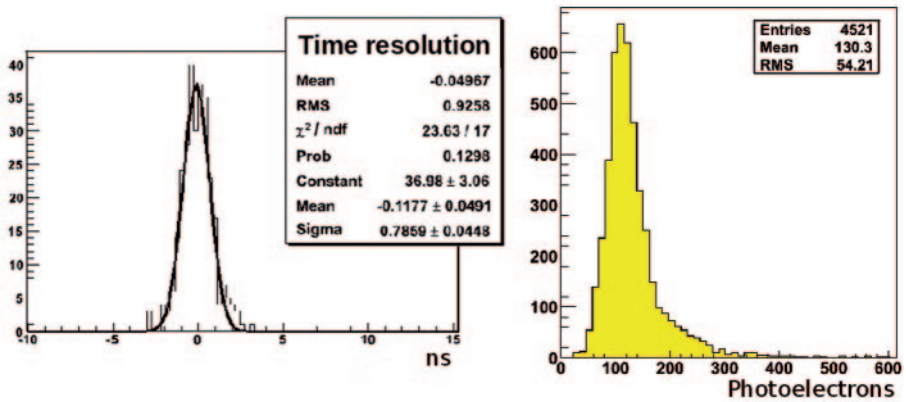

Fig. 7. – Left: Time distribution with time-slewing correction. Right: Collected photo-electrons in two neighbors bars. It corresponds to a cosmic ray crossing about 1.7 cm of scintillator.

TABLE I. – *Fractions of event that pass the cuts. It is normalized to the events that pass the preselection cut.*

Cut	Ratio
Quality	0.505 ± 0.008
Signal Selection	0.021 ± 0.002
CHANTI	0.015 ± 0.001
Quality+Signal Selection	0.0017 ± 0.0006
Quality+CHANTI	0.009 ± 0.001
Signal Selection+CHANTI	0

6. – The CHANTI rejection factor

The most harmful beam interactions are the ones with the GTK station 3. Indeed, they are close to the fiducial volume and the GTK response could be potentially blind to them, especially to that occurred in the last part of the silicon. We use the NA62 Monte Carlo framework, based on GEANT4 package [18], to estimate the CHANTI efficiency on this events.

In this preliminary simulation, we included the GTK, CHANTI, LAV, STRAW and the RICH. For the GTK we used only the information about the reconstructed K momentum (no reconstructed energy deposit) while for the STRAW the full reconstruction was taken in account. Other detectors were implemented by MonteCarlo truth; however we checked that the contributions we considered were the most relevant. In fact, still with all the discussed limitations, we reproduced the efficiency on the signal with an accuracy below 1%.

The study is based on 2.295×10^8 events, of which only 4181 do inelastic interaction on the GTK3 and pass the Preselection cuts ($\approx 1.8 \times 10^{-5}$), which requires that

- inelastic interaction occurred on the GTK3 (discarding the cases in which there was a new K in the final state with a momentum that differes less then $2\sigma \approx 2\%$ with respect to nominal beam momentum 75 GeV);
- one, and only one, positive track was in the Straw;
- K momentum reconstructed in the STRAW was in the range $15\,\mathrm{GeV}/c < P < 35\,\mathrm{GeV}/c$;
- one, and only one, candidate was in the GTK reconstruction;
- one, and only one, pion track was in the RICH acceptance by Monte Carlo truth.

In table I the fraction of events that passed several cuts are given. The quality cut is

- minimal checks on the reconstruction algorithm and cut on the χ^2 of the track candidates in the GTK and STRAW,
- cut on the minimum distance between the GTK track and the STRAW tracks.

The Signal Selection cut is

– kinematical rejection [6],

– vertex reconstructed in the fiducial volume.

The CHANTI cut excludes an event if there is an energy deposit greater than 1/3 of the energy released by a MIP in a single channel.

In table I the "Quality+Signal Selection" row represents the fraction of the dangerous events, while the "CHANTI" row show that the CHANTI rejection factor is about 99.5% on the sample that passes the Preselection cut. Table I endorse the guess that the reconstruction quality is quite uncorrelated to our veto, since CHANTI and Quality cuts roughly factorize.

The simulation also show that the CHANTI inefficiency to the event detection is strongly dominated by acceptance: the 88% of the event that pass the CHANTI did non release any energy in it (*i.e.* no track hit the CHANTI).

Unfortunately, we have currently not enough statistics to make any assertions on the correlation with the Signal Selection cut. A larger Monte Carlo production to shed light on these effects is currently on going.

7. – Conclusions

We have designed and tested a detector (CHANTI) based on scintillator bars, wavelength shifting fibers and silicon photomultipliers to reduce the background induced by beam inelastic interactions in the NA62 experiment. We described the design philosophy, the construction procedure and the quality tests we adopted during the assembly of the detector. It is shown that the CHANTI can safely operate in vacuum, reaches a time resolution of less than one nanosecond and is capable to reduce the inelastic background by two orders of magnitude.

REFERENCES

[1] Buchalla G. and Buras J., *Nucl. Phys. B*, **548** (1999) 309.
[2] Battaglia M., Buras A. J., Gambino P. and Stocchi A., (Editors), CERN report CERN 2003-002-corr (hep-ph/0304132).
[3] Buras A. J., Schwab F. and Uhling S., arXiv:hep-ph/0405132.
[4] Artamonov A. V. *et al.* (E949 Collaboration), *Phys. Rev. Lett.*, **101** (2008) 191802. (arXiv:hep-ex/0808.2459).
[5] Ceccucci A. *et al.*, CERN-SPSC-2005-013,SPSC-P-326.
[6] `http://na62.web.cern.ch/na62/Documents/TechnicalDesign.html`.
[7] Beznosko D. *et al.*, *IEEE Nuclear Science Symposium conference record*, **2** (2004) 790.
[8] MINERVA Collaboration, *MINERVA document*, **218-v4** (2006) .
[9] D0 Collaboration, *Nucl. Instrum. Methods A*, **565** (2006) 413.
[10] `http://www.detectors.saint-gobain.com`.
[11] Ronchetti (on behalf of the ALICE Collaboration), *J. Phys. Conf. Ser.*, **160** (2009) 012012.
[12] Buzhan P. *et al.*, *Nucl. Instrum. Methods A*, **504** (2003) 48.
[13] Golovin V. and Saveliev V., *Nucl. Instrum. Methods A*, **518** (2004) 560.
[14] Sadygov Z. *et al.*, *Nucl. Instrum. Methods A*, **504** (2003) 301.
[15] Angelone M. *et al.*, arXiv:1002.3480

[16] Palladino V., *Simulation, realization and test of veto systems for the NA62 experiment*, Università degli studi di Napoli "Federico II", PhD Thesis (2010).
[17] Antonelli A. *et al.*, arXiv:1111.5768.
[18] CERN toolkit, GEANT4, `http://geant4.cern.ch`.